Is there evidence of determinism in droplet detachment within the gas metal arc welding process?

Charles R. Tolle, Randall A. Laviolette, Herschel B. Smartt, Kevin L. Kenney, David P. Pace, John W. James, Arthur D. Watkins, Thomas Wood, and Daphne L. Stoner
Idaho National Engineering and Enviromental Laboratory
P.O. Box 1625
Idaho Falls, ID 83415-2210
USA

Abstract— **For many years, the welding community has assumed that the detachment events within Gas Metal Arc Welding (GMAW) process are stochastically driven. With this in mind, we set out to better understand these mechanisms and what might drive the detachment events. Through the investigation of 6061-Aluminum GMAW, a number of new insights into globular, and spray transfer modes have been found. By using windowed Fourier transform analysis, akin to Wavelet Analysis, we present evidence that the GMAW process undergoes a shift from the globular mode fundamental frequency to its secondary harmonic frequency as the GMAW process shifts from globular to spray mode transfer. This breakdown and shift from primary to secondary fundamental frequencies and its reverse are shown to occur often within the transition-welding mode in aluminum GMAW. Furthermore, there is partial evidence that this shift of fundamental frequency modes from secondary to the third fundamental frequency continues with the transition from the spray to streaming transfer. The evidence for determinism as the driving force behind GMAW detachments is strengthened through chaotic systems analysis, e.g. surrogate testing using ApEn statistics.**

Keywords—**GMAW; Windowed Fourier Analysis; ApEn; Determinism**

I. INTRODUCTION

In gas metal arc welding (GMAW), the use of a consumable electrode results in a degree of coupling between heat and mass transfer. Approximately 80 to 85% of the electrical energy consumed by the process is transferred to the weldment as heat [1]; approximately one-half of this transferred energy is transported as sensible and superheat molten drops of metal [1]. Consequently, the manner in which the molten drops are transferred to the weldment are of interest. An IIW classification of metal transfer listed six different transfer modes for GMAW [2]. More recent convention lists three modes, in the order of increasing current: *short circuiting* transfer, *globular* transfer, and *spray* transfer [12]. This list neglects an additional mode, well recognized by researchers, called *streaming* transfer or *spray-streaming* transfer which occurs at higher current levels. It is also known that *rotating* transfer can occur at even higher current levels [3], but it is seldom seen in normal welding practice. As for this work, we focus on the *globular* and *spray* transfer modes.

This work was supported by the U.S. Department of Energy, Assistant Secretary for Environmental Management; U.S. Department of Energy, Office of Science, Office of Basic Energy Sciences; and U.S. Department of Energy, Office of Industrial Technology under DOE Idaho Operations Office Contract DE-AC07-99ID13727.

Charles R. Tolle is the corresponding author (Email:tollcr@inel.gov; Phone 208-526-1895).

It has long been recognized that the mode of droplet transfer in gas metal arc welding plays an important role in heat and mass transfer of the process. The various modes of transfer have been identified and mapped in parameter space and static models of detachment have been formulated. However, it is only recently that attempts have been made to understand the physical basis for the dynamics of droplet transfer. One of the challenging questions in understanding droplet transfer dynamics is determining if droplet transfer is a deterministic or stochastic process.

In this work, we look at the frequency content of the electrical signals in GMAW to see what information is present about the metal transfer mode. We have chosen to focus on analyzing the voltage measurements between the contact tip to the work piece. In the sections that follow, we outline the experimental setup; show a correlation between Fourier analysis peaks and droplet detachment times; present a comparison between experimental data and a deterministic GMAW model [4],[5]; and present some initial chaotic analysis used to determine if a signal might be from a deterministic process. The process we undertake within this paper provides a guide for investigating determinism within other dynamic processes of interest.

II. ALUMINIUM GMAW EXPERIMENTS

Within the course of several different welding projects, we became interested in sensing the droplet detachment events through simple electrical measurements for possible inclusion within an advanced GMAW control scheme. As we investigated different welding materials, e.g. steel and aluminum, we found that the electrical signals measured within the aluminum process appeared qualitatively cleaner than those for steel. With this knowledge in hand, we decided to focus on gas metal arc welding of 6061 aluminum bead on plate with 4043 filler wire using an industrial grade (100%) Argon gas shield. We tested several basic welding setups with similar results. For the experimental data presented here, we choose the 4043 electrode diameter to be $0.76mm$, the welding travel speed as $10\frac{mm}{s}$, the constant voltage setting as 20 volts, the contact tip to work piece distance as $20mm$, the 6061 base plate as $\frac{1}{4}$ inch sheet, a gas flow rate of $30scfh$, a weld time of 5 seconds, a data acquisition sample rate of 5000Hz, and we allowed the wire feed speed to range throughout the experiments. We chose to focus on analyzing the voltage measurements between the contact tip to the work piece. Our primary welding power supply was a Miller Maxtron 450 CC/CV in constant voltage mode, although we obtained similar results using a Hobart Arc Master 501 power supply. Similarly, our wire feeder was a Miller Spoolmatic 30A air cooled spool gun for the Fourier analysis results presented in Section III and a Miller 60M Series 24V wire feeder for the model comparison given in Section IV. Our data acquisition system and welding setup were controlled via National Instruments data acquisition system using an internally developed software package running on a windows based PC under the LabVIEW programming environment. Overall, there were well over 300 welds made during the project, only a few results being presented here.

III. FFT Based Evidence

In earlier work, Lesnewitch [6] studied the transition from globular transfer to spray transfer and showed that there is a relatively sharp transition from globular to spray transfer as current is increased. Subsequently, Clark, et. al. [7] studied the transition region between globular and spray transfer, and determined that there is actually mixed mode transfer occurring in this region. Specifically, they determined that a globular transfer event is followed by a series of spray transfer events followed by a globular transfer event, and so on. There is an associated change in arc length. The arc length decreases as the globular drop grows, rapidly increases in length following its detachment, and then decreases slowly in length as the spray droplets transfer until the final droplet in the spray series is stable and grows into the next globular drop. This series continues in a cyclical manner. We noticed this same effect within this work as we viewed the welding processes via our high speed laser back lighting system, sampled at 1000 frames a second. Furthermore, we wondered if these effects of a changing droplet detachment frequencies would be prevalent within the measured contact tip to work piece voltages that we could easily monitor. Therefore, we hand counted droplet detachment events from video footage of each weld to determine both the droplet transfer mode as well as the droplet transfer frequency, see Table I. With the goal of finding the droplet frequency from within the measured voltages, we chose to employ a Fast Fourier Transform (FFT) to break the voltage signal down into its sinusoidal spectral components. This analysis was completed for each of the welds. Example FFTs for each region are show in Figures 1, 2, and 3. The closest significant spectral peak calculated from the FFTs for each weld is listed in Table I. The peak detection algorithm is not presented here, however it is based on a simple smoothing filter applied to the FFT (which could result in a slight shift of the detected frequency) and a simple critical point detection method, i.e. the first and second derivatives. As one studies these FFTs, there seems to be an initial droplet detachment frequency band of 20 to 100Hz for globular transfer with a second harmonic band that appears to grow as one approaches the transition region. During transition the spectral components become blurred across the primary and secondary harmonics within the FFT. As one appears on the spray side there appears to be the establishment of what was the second harmonic mode during globular transfer now acting like a new primary harmonic mode

TABLE I

Tabulation of the hand counted detachment frequencies and FFT peaks for aluminum GMAWs with wire feed speed between $119.1\frac{mm}{sec}$ and $326.1\frac{mm}{sec}$.

GMAW Transfer Mode	Average Voltage	Average Current	Wire Feed Speed	Hand Counted Frequency	FFT Peak Detection
units	Volts	Amps	$\frac{mm}{sec}$	Hz	Hz
globular	24.08	77.32	119.1	22.1	53.4
globular	23.93	83.55	131.9	38.0	65.9
globular	23.62	93.87	151.4	62.2	81.8
globular	23.38	101.95	171.6	85.6	83.3
transition	22.94	120.23	194.1	157.7	172.1
transition	22.74	127.14	206.1	162.3	184.3
transition	22.67	129.87	211.5	204.1	199.6
spray	22.68	129.70	214.2	215.5	214.6
spray	22.41	140.36	234.0	263.2	257.3
spray	22.14	149.45	252.7	306.7	314.7
spray	21.90	156.83	272.5	333.3	338.5
spray	21.67	164.27	291.7	403.2	389.7
spray	21.41	172.39	311.3	406.5	432.2
spray	21.22	178.11	326.1	454.5	445.0

along with its appropriate second harmonic and so forth. We found for our experiment, that the spray frequency band was from about 200 to 500Hz. Although our wire feeder was not able to go any faster, we feel that the growth and power equalization of the spray's primary and secondary harmonic peaks was signaling the approach of the next transition to streaming transfer. However, this conjecture is further strengthened by our ApEn analysis presented in Section V.

In order to further clarify the interactions between the primary and secondary harmonics during transition we considered employing a wavelet transform analysis. However, since this analysis is primarily logarithmic within the frequency bands, it would not allow for the right level of resolution with this problem. Therefore, we choose a simple windowed FFT analysis shown in Figure 4. Within this analysis one can better see the shifting between the globular and spray modes towards the end of the weld, from 3 cm to 5.5 cm. Note the strong reoccurring shifts between spectral components about 100Hz and 150Hz.

IV. Deterministic Model Comparison with Experimental Data

In an effort to obtain a better understanding of metal transfer in GMAW, models of the process have been developed including work by Quinn and Madigan [8], Bingul, et. al. [9], and work at our laboratory [10] and [11]. In Watkin's work, we followed the lead of Shaw [3] on formulation of a dynamic model of water droplets, adding to his model the various additional forces occurring in GMAW, including surface tension, aerodynamic drag by the plasma, electromagnetic forces, and momentum transfer from the electrode. The resulting lumped parameter droplet model was embedded in an electrical model of the secondary circuit of a welding machine, giving a dynamic solution of droplet transfer. This model was later linearized by Moore, et. al. [4],[5]. This linearized version of the model was used to compare deterministically generated detachment time versus wire feed speed plots to experimentally measured detachment time versus wire feed plots, see Figure 5. The model constants used for this comparison are given in Table II. As for the exper-

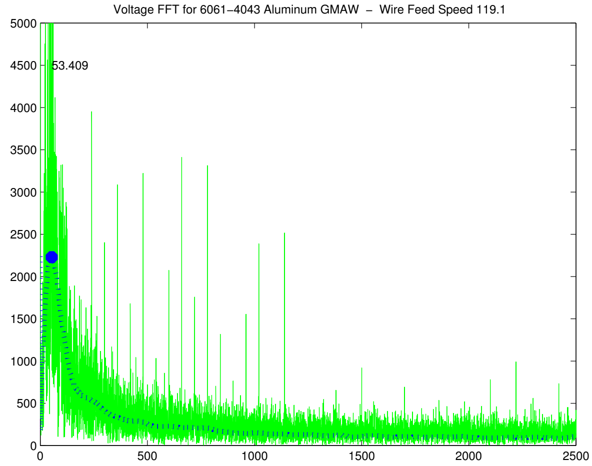

Fig. 1. FFT of voltage signal for globular transfer mode with the wire feed speed 119.1 $\frac{mm}{sec}$, hand counted detachment frequency of 22.1Hz.

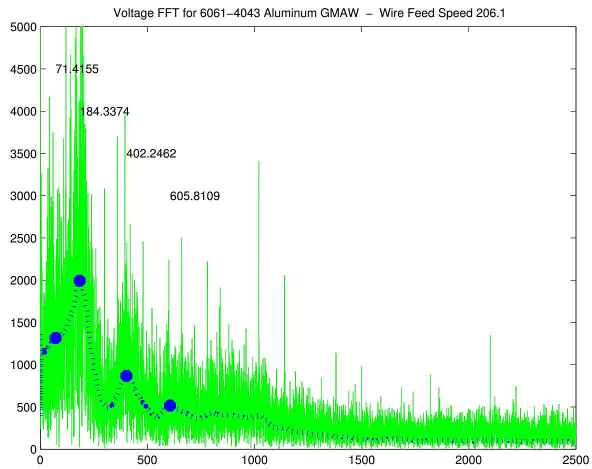

Fig. 2. FFT of voltage signal for transition transfer mode with the wire feed speed 206.1 $\frac{mm}{sec}$, hand counted detachment frequency of 162.3Hz.

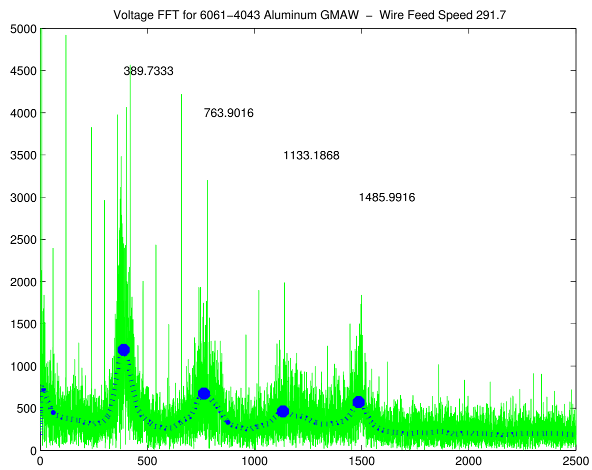

Fig. 3. FFT of voltage signal for spray transfer mode with the wire feed speed 291.7 $\frac{mm}{sec}$, hand counted detachment frequency of 403.2Hz.

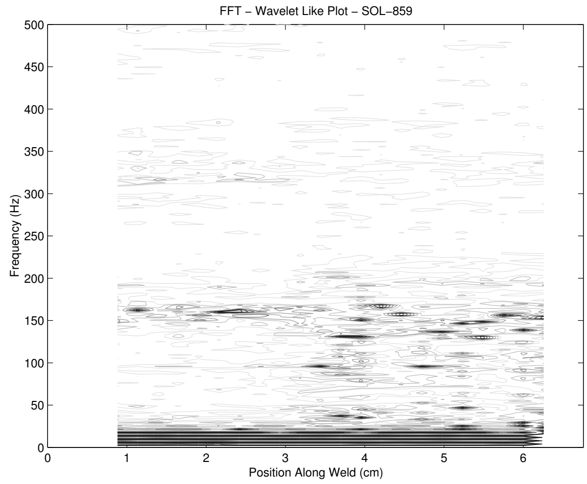

Fig. 4. Windowed FFTs (a poor man's wavelet analysis) of voltage signal for transition transfer mode with the wire feed speed 206.1 $\frac{mm}{sec}$, hand counted detachment frequency of 162.3Hz.

imental detachment times, these were generated using a simple hand-tuned algorithm that predicts droplet detachments using only the time varying voltage signals measured during the welding process. This algorithm was hand-tuned by synchronizing video detachment events with the algorithms predicted detachment events. The algorithm used was:

Initialize the algorithm

$$\bar{v} = \frac{1}{N}\sum_{k=1}^{N} voltage(k) \tag{1}$$

$$\hat{v} = \frac{1}{N-1}\sum_{1}^{N}(voltage(k) - \bar{v})^2 \tag{2}$$

$$\mathcal{T} = \bar{v} + \hat{v} * 1.25 \tag{3}$$

$$\delta t = 0 \tag{4}$$

$$i = 1 \tag{5}$$

repeat
  if $((voltage(i) > \mathcal{T})\ \&\ (voltage(i+1) < \mathcal{T})\ \&\ (\delta t > 5))$
    δt = 0
    Detachment Event
  else
    $\delta t = \delta t + 1$
    No Detachment Event
  end
until $i = N$

Notice that the deterministic model does in fact reproduce the experimental data's qualitative nature quite well (Figure 5). Moreover, note that the quantitative results are quite good as well. It should be noted that this simple linear model is of only 5th order. This will become more important as we investigate the process' *true* order via a couple chaotic analysis tools in Section V.

V. Chaos Toolbox Evidence

As a further step in our quest to determine the motivation for droplet detachment, i.e. stochastic or deterministic, we turn to chaos analysis techniques, as well as hypothesis testing [13]-[15]. It should be noted that these techniques will not definitely

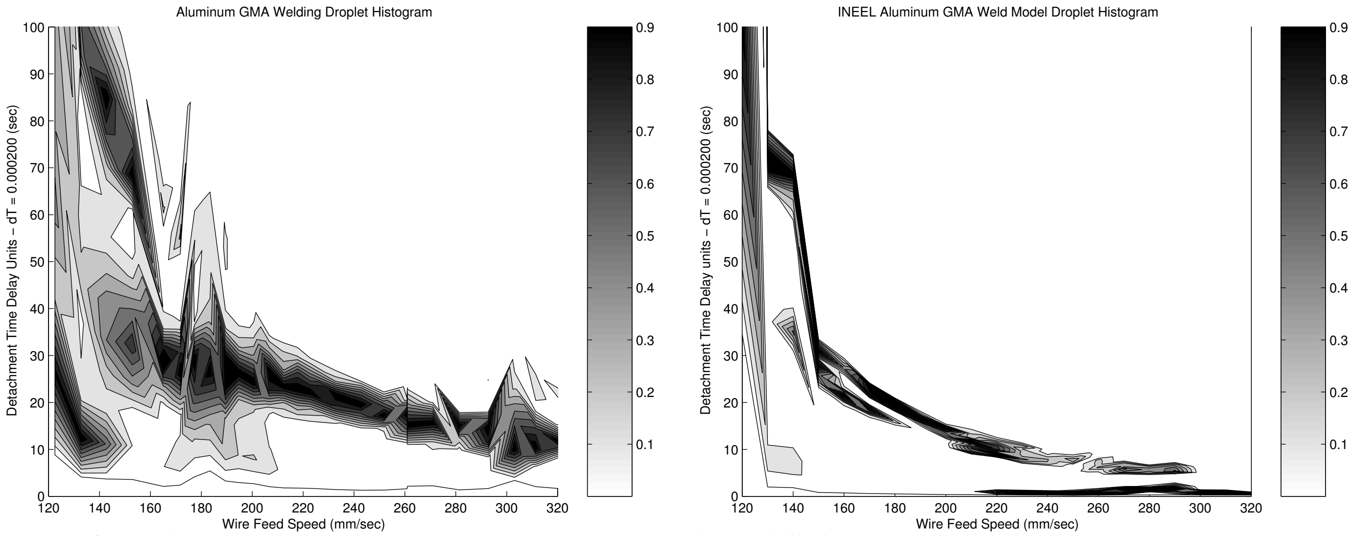

a) Experimental GMAW Data b) Modelled GMAW Data

Fig. 5. Detachment times versus wire feed speed for both experimental and modelled setup.

TABLE II
CONSTANTS USED TO PRODUCE FIGURE 5 B) WITH OZCELIK ET. AL'S DETERMINISTIC GMAW MODEL.

Variable Name	Value	Physical Property
a	0.641	Lorenz force constant
b	1.15	Lorenz force constant
c	0.196	Lorenz force constant
K	0.38	Spring constant
B	1e-6	Damping coefficient
rho	6.2e-2	Resistivity of the electrode
rhow	2700	Electrode density
rhop	1.6	Plasma density
muo	1.25664e-6	Permeability of free space
gama	0.86	Surface tension of liquid aluminum
Ls	0.14e-3	Source inductance
Ra	0.023	Arc resistance
Rs	0.004	Source resistance
Ub	10	Relative fluid to drop velocity
Vo	16.645	Arc voltage constant
Ea	341.54	Arc length factor
rw	3.8e-4	Electrode radius
C1	7.09e-10	Melting rate constant
C2	5.83e-10	Melting rate constant
Cd	0.44	Drag coefficient
g	9.81	Gravity
d1	4πrhow	Constant defined in reset condition
d2	$2\pi^2$gama	Constant defined in reset condition

state if a signal's motivation is stochastic or deterministic, however they do provide a means to rule out large classes of stochastic processes. Similarly, they also provide a means to determine if one cannot statistically tell the difference between the signal of interest and a particular class of stochastic processes, e.g. autoregressive moving average (ARMA) models . The class of stochastic process that most engineers are interested in are easily modelled by linear time invariant systems driven by white noise processes. This is the same class of stochastic processes that we are interested within this work.

Many of these ideas have emerged from the study of topology, functional mappings, and sample theory. The first step in employing the chaotic analysis toolbox is to determine the optimal sampling time for investigating the dynamics within the signals of interest [13],[16]. To do this we have chosen to use mutual information theory [13]. Since chaos analysis tools require a **large** number of data points in general, we generated three additional welds for these types of analysis, i.e. they were each in the globular, transition, and spray regions. These welds lasted 122 seconds. They where sampled at 25000Hz and their wire feed speeds were $170\frac{mm}{s}$, $205\frac{mm}{s}$, and $250\frac{mm}{s}$, respectively. The idea in choosing the right analysis time is that one wants the dynamics to change as much as possible between each time step without losing the correlation to the current time step, i.e. choose the first minimum value within the mutual information curve, see Figure 6. For globular and spray this is about 55 samples or 455Hz. As for the transition mode this is about 70 samples or 360Hz. Clearly, we have vastly over sampled our signal, but this will not effect the analysis presented here. Using these embedding times we applied the false nearest neighbors (FNN) analysis to determine a bound on the dimension of the system, see Figure 7. Note that the FNN analysis bounds the system's order between 3rd and 6th order, i.e. the upper bound come from where the FNN curve drops to zero, and the lower bound comes from Taken's embedding theorem. Moreover, the determination of the 6th order upper bound defines the order of any empirical model developed from this data [13], and it ensures that any phase space reconstructions are untangled. For stochastic signals the FNN analysis tends to approach zero then begins to grow again as the embedding dimension is increased, but this is not the case in Figure 7 for any of the modes. Now that we have an upper bound for the system's order, we can use an estimate of the system's Lyapunov spectrum to determine the system's *true* dynamic order [13]. In doing this we calculate the forward and reverse Lyapunov exponents, see Figure 8. If the forward and reverse exponents converge then that exponent is determined to be real [13]. Moreover, Abarbanel suggests that a zero exponent implies the signals comes from a set of dif-

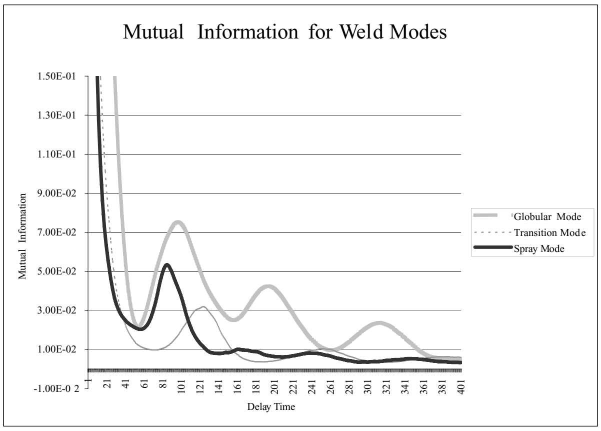

Fig. 6. Mutual information time delay analysis of global, transition, and spray modes for Aluminium GMAW experimental data.

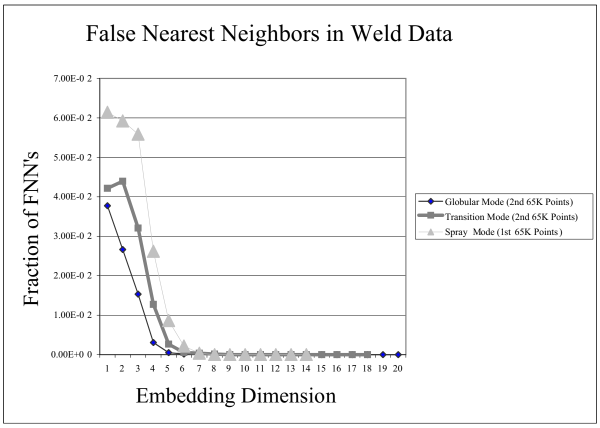

Fig. 7. False Nearest Neighbors (FNN) analysis of global, transition, and spray modes for Aluminium GMAW experimental data.

ferential equations [13]. The reader should be aware that this Lyapunov analysis, while tentative, does suggest that the 5th order model discussed in Section IV seems to be in line with this result.

Finally, we apply an ApEn analysis to a much larger series of welds to infer their detachment motivation, i.e. the same welds used in Figure 5. This analysis consists of three steps: first, a noise reduction of the data, second, the calculation of ApEn for each time series, and finally, the comparison of ApEn of each original time series with ApEn of an ensemble of its surrogates. The techniques employed here closely follow those discussed in detail in Ref.[15].

The noise reduction of the voltage time series was motivated by the observation that only the spikes of about $200V$ were due to droplet detachment; the signals at low voltages were due to fluctuations induced by pre-detachment droplet dynamics. First, each time series was divided into blocks of 200 points. The mean $\overline{V}_B$ and the standard deviation σ_B were calculated for each block. Then the reduced-noise series V_t' was constructed by setting $V_t' = 0$ whenever the corresponding $V_t < \overline{V}_B + 2\sigma_B$, and setting $V_t' = V_t - \overline{V}_B$ otherwise. Thus any non-stationarity that might have been present in the original series was practically eliminated in V_t', an important consideration for the surrogate data analysis discussed below.

The regularity statistic ApEn was calculated for each V_t' time

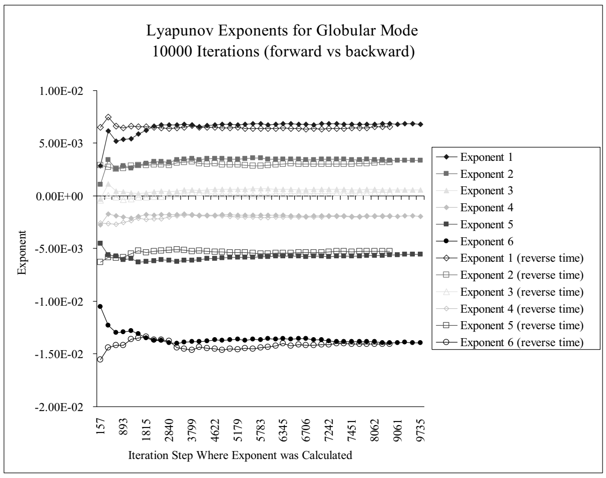

Fig. 8. Lyapunov spectrum analysis of global, mode for Aluminium GMAW experimental data.

series[†]. ApEn ranges from 0 for a perfectly regular (or periodic) time series to $\ln(10) \approx 2.3$ in the limit of an infinitely long uniformly random base-10 time series; lower ApEn corresponds to a more regular (and more correlated) time series. Each series V_t' consisted of 19800 evenly sampled points. We calculated ApEn twice, once for a segment of 8192 points on the left side of the time series, beginning at the origin, and once for the right side, with no points in common. The results are displayed in Figure 9. With no prior knowledge of the physics of the data, ApEn clearly identifies at least three regions as a function of wire feed speed, which correspond to the previously identified globular, transition, and spray regions, respectively. Furthermore, the globular region corresponds to the most regular (low ApEn) time series, while the spray region corresponds to the most irregular time series (higher ApEn), although far from random, consistent with the identification of the regions presented above.

The application of ApEn to the time series is interesting in its own right. Nevertheless, the surrogate data analysis with ApEn provides information concerning the dynamics of the series themselves. As discussed elsewhere[17][18], the surrogate data methods consists of testing the (null) hypothesis that a stationary time series could have been generated from linear stochastic (i.e., ARMA) dynamics by first generating surrogate time series of the original according to simple criteria. If the value of some statistic of the original series were statistically close to the values of the same statistic applied to the surrogates, the null hypothesis would be true. Nonlinear dynamics are a prerequisite for chaotic dynamics, so violations of the null hypothesis are intriguing for stationary time series[‡]. We employed the TISEAN software package to generate surrogates[19], and employed ApEn as the statistic[15], to study a few, representative time series. The results are also incorporated into Figure 9. The only time series studied that displayed a statistically significant violation were for wire feed speeds corresponding to the globular region[§].

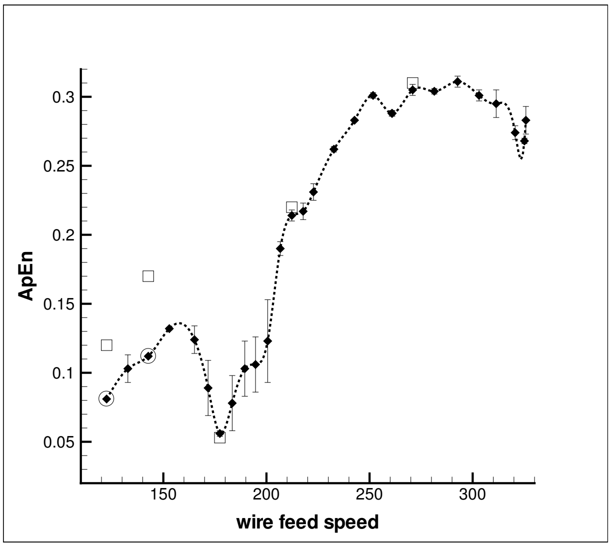

Fig. 9. ApEn vs. wire feed speed The solid diamonds indicate the mean ApEn for the original time series, the error bars indicate its uncertainty estimate, and the dashed curve is a spline to guide the eye. The center of the squares represent the mean ApEn of the surrogates of selected time series, and their height represents a 2σ estimate of its uncertainty. The two circled data points indicate that the null hypothesis is violated at the 5% level. The null hypothesis passes for the others, where the overlap between the original and surrogate ApEn is visible.

VI. Conclusions

Although the evidence is not complete or conclusive, we feel that the new evidence presented here suggests that the droplet detachment process within GMAW appears to be deterministically driven rather than a purely stochastically driven, as previously believed by the community at large.

References

[1] Watkins, Arthur D., *Heat Transfer Efficiency in Gas Metal Arc Welding*, Thesis, University of Idaho, 1989.

[2] Lancaster, J. F., The Physics of Welding, International Institute of Welding, Pergamon Press, New York, ISBN 0-08-030554-7, 1984, p. 210, Table 7.1.

[3] Lancaster, J. F., The Physics of Welding, International Institute of Welding, Pergamon Press, New York, ISBN 0-08-030554-7, 1984.

[4] Moore, K. L., Naidu, D. S., Yender, R. F., Tyler, J., Ozcelik, S., "Experimental Calibration of an Automated GMAW Model", *Trends in Welding Research*, ASM International, ISBN 0-87170-627-X, pp. 314-319, 1998.

[5] Selahattin Ozcelik, Kevin L. Moore, and Subbaram D. Naidu, "Application of MIMO Direct Adaptive Control to Gas Metal Arc Welding," Proceedings of the American Control Conf., Philadelphia, PA, June, 1998.

[6] Lesnewich, A., "Control of Melting Rate and Metal Transfer in Gas-shielded Metal-arc Welding, Part II - Control of Metal Transfer", Welding Journal, pp. 418-s to 425-s, 1958.

[7] Clark, D. E., Buhrmaster, C. L., and Smartt, H. B., "Drop Transfer Mechanisms in GMAW", *Recent Trends in Welding Science and Technology*, ASM International, ISBN 0-87170-372-6, pp. 371-375, 1990.

[8] Quinn, T. P. and Madigan, R. B., "Dynamic Model of Electrode Extension for Gas Metal Arc Welding", *International Trends in Welding Science and Technology*, ASM International, ISBN 0-87170-476-5, pp. 1003-1008, 1993.

[9] Bingul, Z., Cook, G. E., Barnett, R. J., Strauss, A. M., Wells, B. S., "An Investigation of Constant Potential GMAW Instability Behavior", *Trends in Welding Research*, ASM International, ISBN 0-87170-627-X, pp. 289-294, 1998.

[10] Watkins, A. D., Smartt, H. B., and Johnson, J. A., "A Dynamic Model of Droplet Growth and Detachment in GMAW", *International Trends in Welding Science and Technology*, ASM International, ISBN 0-87170-476-5, pp. 993-997, 1993.

[11] Murray, P. E., "Stability of a Pendant Droplet in Gas Metal Arc Welding", *Trends in Welding Research*, ASM International, ISBN 0-87170-627-X, pp. 308-313, 1998.

[12] R. L. O'Brien, editor, *Welding Handbook*, 8th edition, vol 2, "Welding Processes", American Welding Society, 1991.

[13] Henry D.I. Abarbanel, *Analysis of Observed Chaotic Data*, Springer-Verlag New York Inc., New York, NY, 1996.

[14] Steven H. Strogatz, *Nonlinear Dynamics and Chaos - With application to Physics, Biology, Chemistry, and Engineering*, Addison-Wesley Publishing Company, Reading, Main, 1994.

[15] R. A. LaViolette, T. R. McJunkin, C. R. Tolle, and D. L. Stoner, "Surrogate data analysis of staionary time series employing ApEn statistics," preprint, submitted to Applied Math. Modell., February 2002.

[16] C. R. Tolle, and R. W. Gundersen, "Searching for Determinism in Erratic Signals: Fuzzy Time-Based Clustering of Delay Vectors," *Intelligent Engineering Systems Through Artificial Neural Networks: Volume 8, Smart Engineering Systems: Neural Networks, Fuzzy Logic, Evolutionary Programming, Data Mining, and Rough Sets*, Eds. Cihan H. Dagli et. la., ASME Press, New York, NY, 1998.

[17] J. Theiler, S. Eubank, A. Longtin, B. Galdrikian, and J. D. Farmer, "Testing for nonlinearity in time series: the method of surrogate data", *Physica D* **58** (1992) 77.

[18] H. Kantz and T. Schreiber, Nonlinear Time Series Analysis, (Cambridge University Press, New York, 1997).

[19] R. Hegger, H. Kantz, and T. Schreiber, "Practical implementation of nonlinear time series methods: The TISEAN package", *Chaos* **9** (1999) 413; T. Schreiber and A. Schmitz, "Surrogate time series", *Physica D* **142** (2000) 346. The software is freely available at `www.mimpks-dresden.mpg.de/~tisean/TISEAN_2.1/index.html` We employed the iteration scheme that employs the default convergence criterion, i.e., it stops when the amplitudes of the original and the surrogates agree within a certain tolerance.

Endnotes

[†] ApEn is a statistic devised by Pincus (cf. S. M. Pincus, "Approximate entropy as a measure of system complexity", *Proc. Nat. Acad. Sci.* **88** (1991) 2297; S. M. Pincus, "Approximate entropy (ApEn) as a complexity measure", *Chaos* **5** (1995) 110;S. M. Pincus and B. H. Singer, "Randomness and degrees of irregularity", *Proc. Nat. Acad. Sci.*) to measure the regularity, and by extension, the complexity of a sequence. Specifically, ApEn is the conditional probability that runs of patters that are close for some number of observations remain close. ApEn for finite data depends primarily upon three parameters that need to be held constant for the sake of meaningful comparison: N, the length of the time series, m, the length of the test pattern, and a tolerance r that defines the closeness of patterns. In certain limits ApEn is related to the topological and the metric entropy, thus ApEn is "approximate entropy", but we follow Pincus' suggestion to employ ApEn as a statistic in its own right. Also following Pincus' recommendations, we fix $N = 8192$, $m = 2$, and $r = 0.2\sigma$, where σ is the standard deviation of the time series V_t'.

[‡] It has been pointed out that a non-stationary time series constructed with simple linear stochastic dynamics also gives a violation of the null hypothesis. See J. Timmer, "The power of surrogate data testing with respect to non-stationarity", *Phys. Rev. E* **58** (1998) 5153.

[§] As discussed in Ref.[15], we employed the two-sided Wilcoxson rank sum test at the 5% significance level. See also R. L. Schaeffer and J. T. McClave, Probability and Statistics for Engineers, Third Ed., (PWS-Kent, Boston, 1990); Ch. 12.